

Modeling the detectability of cavities under rebar structures in case of GPR measurements

Introduction

Ground-penetrating radar (GPR) is a non-destructive geophysical technique that uses electromagnetic (EM) waves to image the near surface. It is widely used for solving geological, geotechnical, archeological, or civil engineering problems. The popularity of the method is thanks to its speed, effectiveness, relatively low cost and reliability. However, GPR has some limitations as well. The main reason is the strong attenuation of GPR waves in the conductive material. For example, the method rarely can be applied successfully in low resistivity environment (e.g. in the presence of clayey wet soils). Resolution and penetration depth are also limited. That is why measurement design must be the first step in the beginning of a GPR project. Forward modeling can be also useful before the on-field GPR survey, especially if there are available information about the area.

Basically, the GPR response depends on the electromagnetic petrophysical properties of the media: conductivity (σ), relative dielectric constant (ϵ_r) and magnetic permeability (μ_r). Beside them, the antenna frequency (wave frequency) influences the wave propagation in the investigated media (Martinez and Byrnes, 2001). In the general GPR practice, dielectric medium is assumed, which is usually correct. The more complex lossy medium assumption describes reality better.

In most cases of GPR practice, the change of magnetic permeability in the investigated media is not typical. The relative magnetic permeability is usually around one ($\mu_r \approx 1$), because ferromagnetic materials are rarely present. But civil engineering practice is a very important branch of GPR applications, where different types of reinforcement bars (rebars) need to be investigated. These steel rebars – which prove the load bearing capacity of the concrete – are ferromagnetic, so their relative magnetic permeability is high.

Theory

Assuming either dielectric or lossy medium, the propagation velocity of the GPR waves decreases very rapidly with increasing relative magnetic permeability (Nádasi and Turai, 2017, 2018). Obviously, it is not surprising looking at the formulas of EM wave propagation velocities:

$$v_d = \frac{1}{\sqrt{\mu\epsilon}} \cong \frac{c}{\sqrt{\mu_r\epsilon_r}}, \quad (1)$$

$$v_v = \left\{ \frac{\mu\epsilon}{2} \left[\left(1 + \frac{\sigma^2}{\epsilon^2\omega^2} \right)^{1/2} + 1 \right] \right\}^{-1/2} \quad (2)$$

The wavelength is also affected by the magnetic permeability change. Thus, the resolution of measurements is also influenced by the presence of ferromagnetic materials:

$$\lambda_d = \frac{2\pi}{\omega} \sqrt{\mu\epsilon}, \quad (3)$$

$$\lambda_l = \frac{2\pi}{\omega} \sqrt{\frac{\mu\epsilon}{2} \left(\sqrt{1 + \frac{\sigma^2}{\epsilon^2\omega^2}} + 1 \right)}, \quad (4)$$

where

- μ is the absolute magnetic permeability of the medium,
- μ_0 is the absolute magnetic permeability of vacuum,
- v_d is the wave propagation velocity calculated in the dielectric,
- v_l is the wave propagation velocity calculated in lossy media,
- ε is the absolute dielectric constant of the medium,
- ε_r is the relative dielectric constant of the medium with respect to vacuum,
- c is the velocity of light in vacuum,
- σ is the specific electrical conductivity of the medium,
- ω is the angular frequency,
- λ_d is the wavelength calculated in the dielectric,
- λ_l is the wavelength calculated in lossy media.

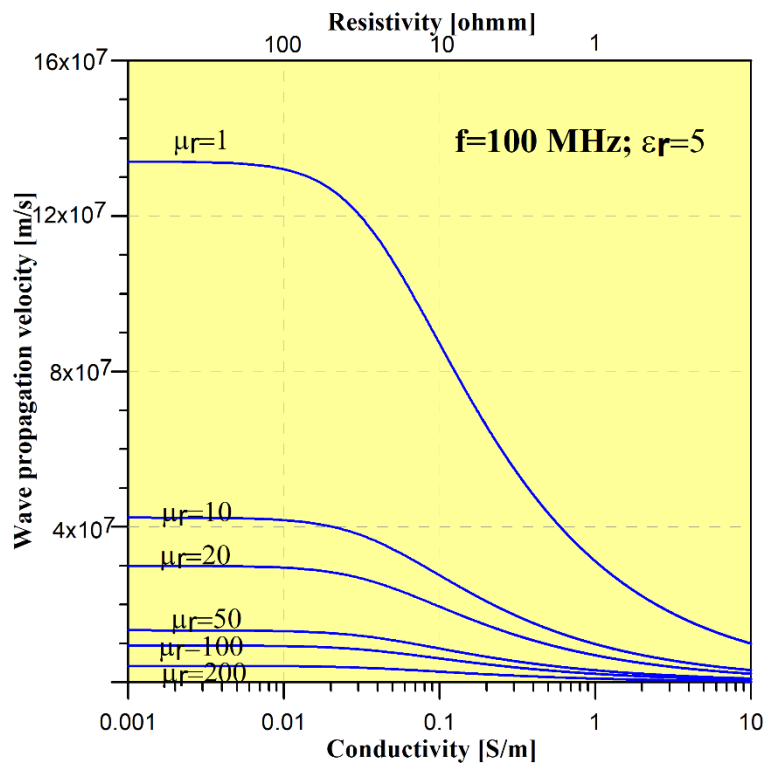


Figure 1 The EM wave propagation velocity as a function of conductivity, in case of increasing relative magnetic permeability, 100 MHz frequency and $\varepsilon_r=5$ relative permittivity.

Figure 1 shows the characteristics of this decreasing velocity trend. The highest permeability value on the figure ($\mu_r=200$) is still very far from existing ferromagnetic values ($\mu_r>1000$). In ferromagnetic materials, the velocity may be even one order of magnitude lower. In case of steel rebars, the relative permeability (μ_r) is about 100 and the electrical resistivity (ρ) is around $10^{-6} \Omega\text{m}$. These values have been used in the modeling examples. The permeability of ferromagnetic materials are nonlinear, they show saturation and hysteresis.

Modeling examples

For forward modeling the MATGPR system (Tzani, 2010) was used. The synthetic GPR sections were calculated with the method of Bitri and Grandjaen (1998).

In the modeling example presented below (Figure 2) the background was set to the following EM parameters: $\rho=500 \Omega\text{m}$; $\varepsilon_r=9$; $\mu_r=1$. The rebars were set to the same diameter ($d=1$ cm) in

10 cm depth, 20 cm from each other, their parameters: $\rho=10^{-6} \Omega\text{m}$; $\epsilon_r=2$; $\mu_r=100$. The rectangle-shape (40 x 20 cm) cavity in 50 cm depth has $\rho=10^4 \Omega\text{m}$; $\epsilon_r=1$; $\mu_r=1$.

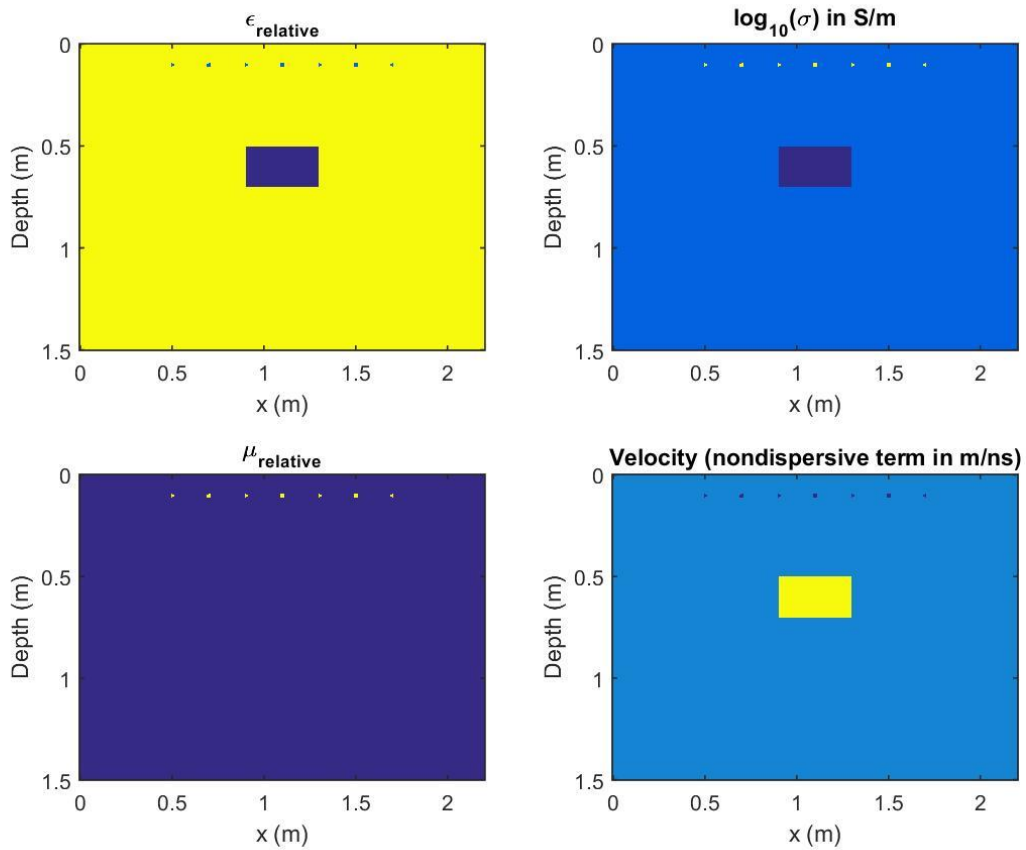


Figure 2 Simple 2D model with 10 cm diameters rebars and a cavity underneath. The different colors illustrate the distribution of the EM parameters.

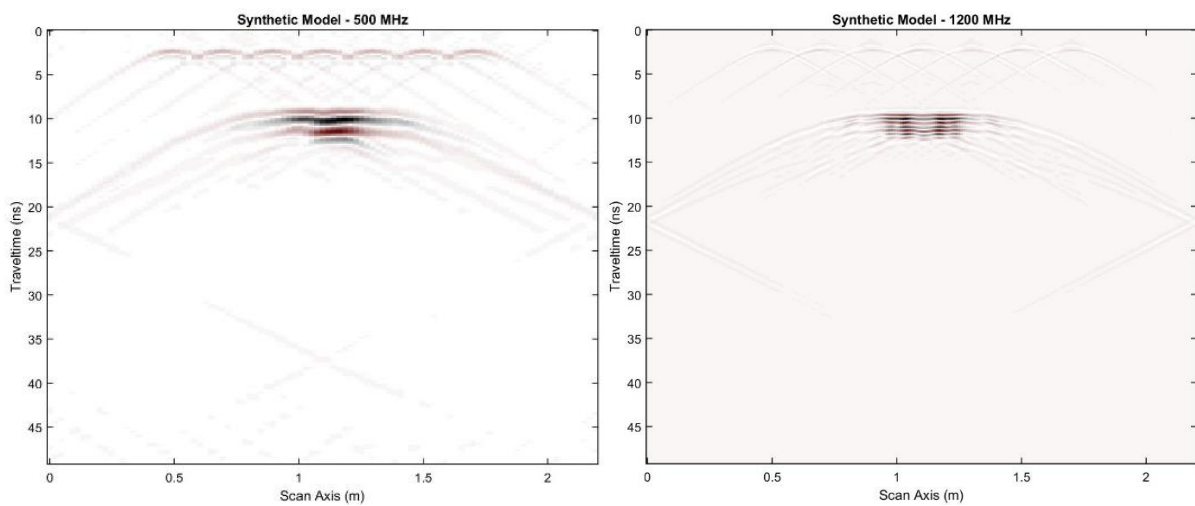


Figure 3 Synthetic radargrams of the 2D model of Figure 2. Each rebar produced one separable hyperbole, the cavity is also easily detectable at both (500 MHz and 1.2 GHz) frequencies.

The synthetic models show that all the seven rebars appear with strong reflections, so they can be detected easily in a concrete structure. In the presented case, the difference between the two frequencies is the resolution. Thus, the amplitudes are also different on the two images. The most remarkable sign is that the less visible rebars on the high frequency radargram. The rebar can overshadow an anomaly underneath. However, cavities can be detected even below the rebar, as Figure 3 shows. Some straight reflection lines appear on the radargrams which are caused by the side effect of the modeling domain (reflections from the edges).

Conclusion

The GPR measurement of rebar structures is a challenging task. The antenna frequency must be chosen carefully to get good resolution images. Because the EM waves attenuate intensively and their velocity decreases significantly in ferromagnetic materials, good resolution is not hopeless under a rebar structure. Moreover, the rebar structure itself can be monitored accurately if the measurement is well prepared. The forward modeling of the expected structure will increase the possibility of a successful GPR measurement. A model series has been produced to model real practice situations. The model series contains a set of several values of the parameters (size and depth of cavity and rebars, distance of rebars, EM petrophysical parameters: ϵ, ρ, μ).

Detecting additional anomalies around the rebar structure is an interesting and complex modeling problem. Since weak and normal anomalies may stay hidden under the rebar system, strong anomalies can be still recognized in this environment. To refine the model series – creating more accurate and realistic rebar geometries – and to involve real field data to the interpretation is the next step of this research.

Acknowledgements

The research was funded by the Project No. K-135323 supported by the National Research, Development and Innovation Office (NKFIH), Hungary.

References

- Bitri, A. and Grandjean, G., 1998. Frequency - wavenumber modelling and migration of 2D GPR data in moderately heterogeneous dispersive media, *Geophysical Prospecting*, 46, 287-301.
- Martinez, A., & Byrnes, A. P. (2001). Modeling dielectric-constant values of geologic materials: An aid to ground-penetrating radar data collection and interpretation. *Current Research in Earth Sciences, Bulletin 247*, part 1.
- Nádasi, E. and Turai, E.: Analysis of electromagnetic petrophysical parameters in GPR survey (in Hungarian). *MAGYAR GEOFIZIKA* 58 : 4 pp. 253-258. , 6 p. (2017)
- Nádasi, E. and Turai, E.: Increasing the accuracy of GPR measurements. *GEOSCIENCES AND ENGINEERING: A PUBLICATION OF THE UNIVERSITY OF MISKOLC* 6 : 9 pp. 142-150. , 8 p. (2018)
- Tzani, A., 2010. matGPR Release 2: A freeware MATLAB® package for the analysis & interpretation of common and single offset GPR data, *FastTimes*, 15 (1), 17 – 43.